SIMULATION OF LANDSAT THEMATIC MAPPER IMAGERY USING AVIRIS HYPERSPECTRAL IMAGERY

Linda S. Kalman and Gerard R. Peltzer

The Aerospace Corporation
P.O. Box 92957
Los Angeles, CA 90009-2957

1. INTRODUCTION

In this paper we present a methodology for simulating multispectral imagery (MSI) using hyperspectral imgery (HSI), and present a validation of the technique using one nearly coincident Landsat TM and AVIRIS data set. Generation of MSI from HSI supports several investigations including selection of multispectral sensor band edges, and engineering trade studies related to on-board or ground-based aggregation of HSI to simulate MSI. In addition, the utility of this technique as a potential procedure for monitoring calibration changes in spaceborne instruments is also addressed.

2. SIMULATION METHODOLOGY

The signal, Se, (in electrons) in a selected waveband of a multispectral sensor is given by :

$$Se = K \int R(\lambda)\ F(\lambda)\ \lambda / hc\ d\lambda \qquad (1)$$

where $R(\lambda)$ represents the sepctral radiance distribution at the sensor aperture, $F(\lambda)$ is the combined spectral responsivitiy of the sensor (including spectral filter response, detector spectral responsivity, etc.), and K represents an assortment of wavelength independent components including sensor aperture solid angle, integration time, detector size, etc. The conversion between photons and electrons is represented by the term λ/hc. The integration is performed over the spectral bandpass of the band in question.

The process of inverting equation (1), eg. the estimation of $R(\lambda)$ from a measured signal does not have a unique solution. Instead, one may estimate the equivalent radiance, Re, ie. the spectrally flat radiance distribution which when used in equation (1) would produce the same measured signal:

$$Se = K \int Re\ F(\lambda)\ \lambda / hc\ d\lambda \equiv K\ Re \int F(\lambda)\ \lambda / hc\ d\lambda \qquad (2)$$

Equating (1) and (2) we have a definition of this equivalent radiance:

$$Re = \int R(\lambda)\ F(\lambda)\ \lambda\, d\lambda \ /\ \int F(\lambda)\ \lambda\ d\lambda \qquad (3)$$

The equivalent radiance, Re, when multiplied by the nominal sensor bandpass, $\Delta\lambda$, is commonly referred to as the "inband" radiance. The relationship between this inband radiance and Landsat digital values, Dn, is defined through the calibration information supplied with Landsat data :

$$Re\ \Delta\lambda = Gain * Dn + Offset \qquad (4)$$

Simulation of Landsat digital data can therefore be accomplished through computation of the inband radiance, $Re\ \Delta\lambda$, followed by application of the appropriate band calibration coefficients.

Calibrated imagery, such as that produced by the AVIRIS sensor is an ideal

candidate for estimation of $R(\lambda)$. Given n hypersperspectral bands spanning the bandpass of the multispectral sensor band being simulated, equation (3) can be approximated as :

$$Re = \sum_{i=1}^{n} R_A(i)\ F(\lambda_i)\ \lambda_i \Delta\lambda_i \ / \ \sum F(\lambda_i)\ \lambda_i\ \Delta\lambda_i \qquad (5)$$

where $R_A(i)$ is the calibrated spectral radiance measured in AVIRIS band i, λ_i is the center wavelength of band i, $\Delta\lambda_i$ is the bandpass of band i, and $F(\lambda_i)$ is the spectral response value of the sensor being simulated at wavelength λ_i. The fidelity with which Re can be generated depends on the calibration accuracy of the hyperspectral imagery and also improves as the number and spectral resolution of the hyperspectral bands covering the bandpass in question increases.

3. EXPERIMENT AND RESULTS

We have investigated the merits of this simulation technique using an AVIRIS scene collected nearly coincident with a Landsat TM scene. The AVIRIS scene obtained on 10/08/90 at 1041 Z, and covers the area surrounding Corvallis Oregon. A Landsat 5 TM scene (geometrically corrected, P type data) was collected on the same day at approximately 1745 Z. Weather reports generated at Eugene (50 miles away) as well as the general appearance of both images indicate a relatively clear, cloud free atmosphere during the acquisitions. The FWHM and center wavelength files accompanying the calibrated AVIRIS imagery were used in equation (3). Preflight measurements of the Landsat sensor spectral response function (Engel,1990) were used as a source for $F(\lambda_i)$. The six reflective bands of the Landsat 5 TM instrument were simulated using equations (3) and (5) along with calibration data found in the TM data header file. (A multiplicative sun angle correction based on the change in solar zenith angle between the two collections was applied to the simulated TM radiances prior to conversion to digital counts.)

3.1 Evaluation of Results

A portion of the TM scene was geometrically warped to overlay the AVIRIS data. A common sub area of the two images was then extracted for statistical analysis. Color composites of the simulated and actual TM scenes are provided in Slide 3. Histograms of the simulated and actual TM bands were computed for the spatially registered areas. A few of the histograms are displayed in Figure 1 and a summary of the scene statistics presented in Table 1. The agreement between simulated and actual scene statistics and histograms is exceptionally good. Both band 4 and band 5 histogram comparisons show the simulated image histograms to be slightly compressed. To investigate the source of this effect we computed statistics for several homogeneous sub areas in the simulated TM imagery and corresponding areas in the unwarped, original TM image. Samples of these results are plotted in Figure 2. Linear relationships between simulated Dn and actual TM Dn were found to exist for each band. The linear regression data are shown in Table 2. Several investigators (including Thome et al, 1993) have observed a decrease in TM response in each band over the course of the years. Since EOSAT has not changed calibration coefficients since 1986, we would expect that use of those coefficients to compute Dn from the radiance derived using the AVIRIS data would yield higher values than the actual digital values observed in the TM scene. Unfortunately, this is not what we observed. This discrepancy suggests that perhaps the AVIRIS calibration for this data set is erroneously low. With only one data set it is difficult to draw decisive conclusions regarding the source of these discrepancies.

In this analysis we have focussed upon the radiometric fidelity of the simulation procedure. A rigorous simulation of multispectral imagery would include an accurate

modeling of electronic and signal dependent noise in the image, as well as modification of the MTF characteristics as appropriate. The spectral band aggregation generally produces the desirable effect of decreasing the noise level in the simulated image. The user is then free to add back in the desired amount of noise expected in the sensor product so long as the individual spectrometer band noise levels are comparable to those of the sensor to be simulated. Furthermore, the aggregation procedure increases the effective bit-resolution of the simulated data, allowing the user to explore design tradeoffs related to bit allocation and digitization schemes. Finally, the accuracy of the simulation is dependent upon the spectral resolution of the HSI. The number of bands actually required will most likely depend on the shape and complexity of the sensor response function being simulated.

3.2 Potential applications of the simulation technique.

Discrepancies between the simulated TM data and the actual TM data can be attributed to calibration errors in either instrument, as well as to the coarseness arising from the limited number of AVIRIS spectral bands covering any given TM band, particularly in the shorter wavelengths. Changes in responsivity for the TM instrument throughout the years have been observed by investigators including Thome et al. (1993). We performed an experiment in which we shifted the long wavelength edge of the TM2 spectral response curve; in effect, changing the effective filter passband. The long edge was shifted from -10 nm to +10 nm from its nominal position. The statistics derived from these experiments are shown in Table 3. It is clear that a change in filter response similar to this could be detected and quantified using imagery simulated from underflights with a hyperspectral sensor such as AVIRIS. We are currently performing analyses to determine if this procedure can be used to identify the exact nature of the change in filter response : eg. to distinguish between shifts at the low or high wavelength end, or both, as well as changes in transmittance due to contamination of the optical surfaces or changes in detector responsivity over time.

4.0 SUMMARY

We have presented a procedure for simulating multispectral imagery using hyperspectral data. The simulation technique is straightforward and has been shown to produce encouraging results in the one case studied, although with only one data set it is impossible to distinguish errors in the AVIRIS calibration or the TM calibration. We are currently in the process of obtaining additional data sets to use in further validation of the procedure. It is clear however, that reasonable simulations of multispectral imagery can be produced using this technique. A simulation technique such as this provides the capability to perform engineering design trades for future multispectral sensors related to determination of spectral band placement. In addition, the analysis technique may be useful as a tool for monitoring changes in calibration of space sensors using aircraft underflights. The sensitivity of this technique for detecting changes in sensor characteristics is currently under study.

5.0 ACKNOWLEDGEMENTS

The authors wish to thank Dr. P. Slater (Univ. of Arizona, Tucson) for his helpful comments and suggestions regarding the course of this work. This work was supported by the Aerospace Sponsored Research program.

6.0 REFERENCES

Engel, J., SBRC (Private Communication).

Thome, K.J., D. I. Gellman, R.J. Parada, S. F. Biggar, P.N. Slater, and M.S. Moran, 1993. "In-flight Radiometric Calibration of Landsat-5 Thematic Mapper from 1984 to Present", Vol. 1938-14, Proc. SPIE, Orlando, Fla. April, 1993.

Table 1. Comparison of Simulated Scene Statistics with Actual Scene Statistics

Band	Simulated Mean Dn	Actual Mean Dn
1	54.3	54.0
2	22.2	22.0
3	24.1	24.0
4	40.3	41.0
5	55.3	57.9
7	24.5	25.8

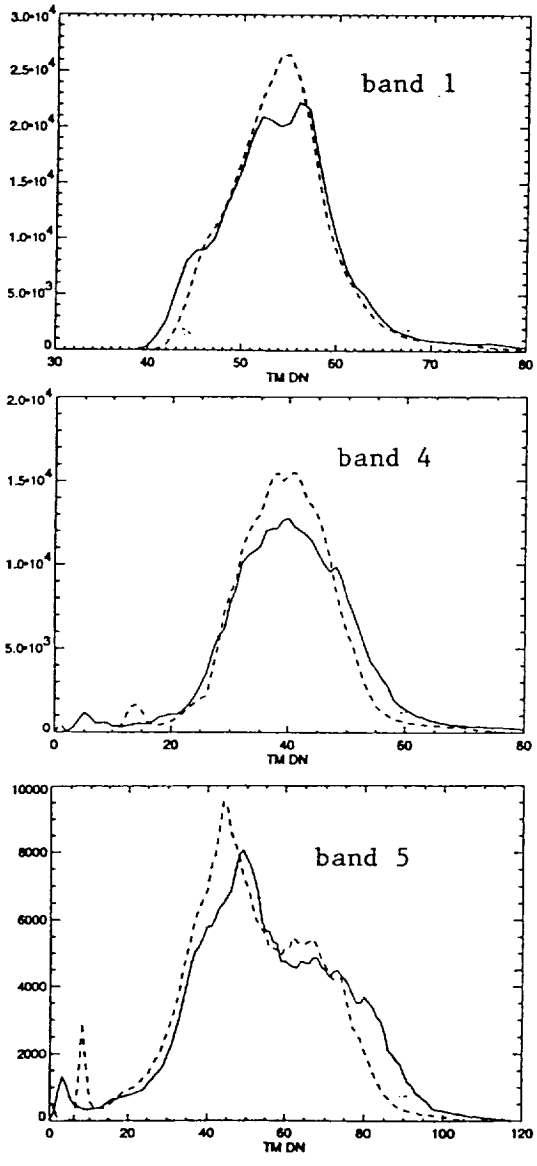

Figure 1. Histogram Plots of Simulated (dotted line) and actual (solid line) TM scenes.

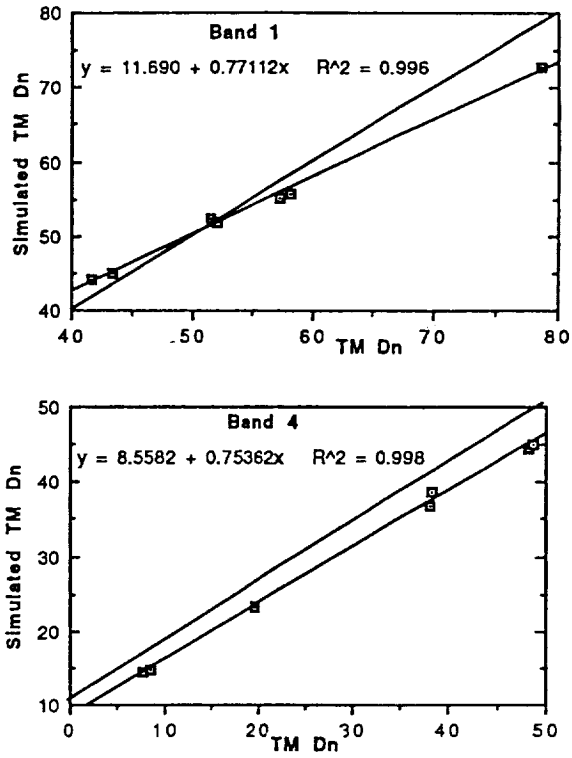

Figure 2. Simulated Dn plotted against actual Dn for corresponding subareas (bands 1 and 4).

Table 2. Equation coefficients describing the relationship between simulated and actual TM values.
Simulated (Y) = Gain * Actual (X) + Offset

Band	Gain	Offset
1	.77	1.69
2	.83	4.58
3	.81	4.94
4	.75	8.56
5	.82	5.65
7	.91	2.31

Table 3. Statistics Derived from Shifting Upper Edge of TM Band 2 response function.

Band	Shift (nm)	Simulated Scene Mean Dn
2	-10	20.5
	- 4	21.9
	0	22.9
	+ 4	23.8
	+10	25.3